VŠB – Technical University of Ostrava
Faculty of Electrical Engineering and Computer Science
Department of Computer Science

The 0-1 test for chaos

0-1 test chaosu

2018 Judita Nagyová

VŠB - Technical University of Ostrava
Faculty of Electrical Engineering and Computer Science
Department of Applied Mathematics

Bachelor Thesis Assignment

Student:	**Judita Nagyová**
Study Programme:	B2647 Information and Communication Technology
Study Branch:	1103R031 Computational Mathematics
Title:	"0-1" test for chaos "0-1" test chaosu
The thesis language:	English

Description:

Dynamic systems are characterized by variety of properties. These properties help us with the understanding of behaviour of all system. One of those properties is chaos. Chaos is standardly checked by different tools in applications. One such new tool is the "0-1" test for chaos.

The main aim of this thesis is to study newly defined the "0-1" test for chaos and verify this test on suitable examples (implementation including).

The tools for the thesis:

1. to study and define all needed notions
2. to construct typical maps of the discrete dynamical systems
3. to apply the "0-1" test for chaos on relevant models
4. to compare outputs of tests with known ones
5. to formulate conclusions

References:

[1] R.L. Devaney, An Introduction to Chaotics Dynamical Systems, Benjamin/Cummings, Menlo Park, CA., 1986.
[2] G. A. Gottwald and I. Melbourne. A new test for chaos in deterministic systems. Proc. Roy. Soc. A 460 (2004) 603–611.
[3] G. A. Gottwald and I. Melbourne. Testing for chaos in deterministic systems with noise. Physica D 212 (2005) 100–110.
[4] G. A. Gottwald and I. Melbourne. Comment on "Reliability of the 0–1 test for chaos". Phys. Rev. E 77 (2008) 028201.
[5] G. A. Gottwald and I. Melbourne. Validity of the 0–1 test for chaos. In preparation.
[6] J. Hu, W. -W. Tung, J. Gao and Y. Cao. Reliability of the 0–1 test for chaos. Phys. Rev. E 72 (2005) 056207.
[7] S. Lynch, Dynamical systems with Applications using Matlab, Birkhauser, 2004, ISBN: 0-8176-4321-4

Extent and terms of a thesis are specified in directions for its elaboration that are opened to the public on the web sites of the faculty.

Supervisor: **doc. RNDr. Marek Lampart, Ph.D.**

Date of issue: 01.09.2017

Date of submission: 30.04.2018

doc. RNDr. Jiří Bouchala, Ph.D.
Head of Department

prof. Ing. Pavel Brandštetter, CSc.
Dean

I hereby declare that this bachelor's thesis was written by myself. I have quoted all the references I have drawn upon.

Ostrava, 30 April 2018 .....

My sincere thanks go to everybody who supported me in writing this thesis, especially my supervisor doc. RNDr. Marek Lampart, Ph.D., for all his help, patience and motivation, without which I would never be able to finish this work.

Abstrakt

Hlavním cílem bakalářské práce je studium 0-1 testu chaosu, jeho implementace v Matlabu a následné testování na vhodných modelech. V práci jsou zavedeny základní nástroje analýzy dynamických systémů, které jsou později použity v části hlavních výsledků. 0-1 test chaosu je podrobně uveden, řádně definován a implementován v Matlabu. Aplikace je provedena na dvou jednodimenzionálních diskrétních modelech z nichž jeden je v explicitním a druhý v implicitním tvaru. V obou případech byly provedeny simulace v závislosti na stavovém parametru a hlavní výsledky byly demonstrovány formou 0-1 testu chaosu, fázových a bifurkačních diagramů.

Klíčová slova: dynamické systémy, 0-1 test chaosu, bifurkační diagram, populační model

Abstract

The goal of this thesis is to research the 0-1 test for chaos, its application in Matlab, and testing on suitable models. Elementary tools of the dynamical systems analysis are introduced, that are later used in the main results part of the thesis. The 0-1 test for chaos is introduced in detail, defined, and implemented in Matlab. The application is then performed on two one-dimensional discrete models where the first one is in explicit and the second one in implicit form. In both cases, simulations in dependence of the state parameter were done and main results are given - the 0-1 test for chaos, phase, and bifurcation diagrams.

Key Words: dynamical systems, the 0-1 test for chaos, bifurcation diagram, population model

Contents

List of symbols and abbreviations **8**

List of Figures **9**

Listings **10**

1 Introduction **11**
1.1 Organization and goals of the thesis 12

2 Preliminaries **13**

3 Overview of the 0-1 test for chaos **15**
3.1 Application on experimental data 15
3.2 Application on discrete dynamical systems 16
3.3 Application on continuous dynamical systems 17

4 Tools of dynamics detection **18**
4.1 The 0-1 test for chaos 18
4.2 Bifurcation diagram 20

5 On implementation in Matlab **21**

6 Application of the test **25**
6.1 Ricker model 25
6.2 Discrete and nonoverlapping generations regulated by microparasites 32

7 Conclusions **39**

References **40**

List of symbols and abbreviations

(X,f)	–	a discrete dynamical system
Fix	–	the set of all fixed points
Per_n	–	the set of all periodic points od period n
MSD	–	mean square displacement

List of Figures

1 Plot of first (on the left) and second (on the right) iteration of the function $R_r(x) = xe^{r(1-x)}$ for different values of the parameter r. 27

2 Cobweb diagram of $R_r(x) = xe^{r(1-x)}$ for $r = 1.5$ (on the left) and $r = 2.5$ (on the right). It shows the fixed point $x_1 = 1$. 28

3 Plot of p versus q for $R_r(x) = xe^{r(1-x)}$, for $r = 3$, $r = 3.15$, $r = 3.6$ and $r = 3.8$ on 20000 data points and 100 equally spaced values of c, $c \in [\pi/5, 4\pi/5]$. The second and third picture shows regular dynamics for $r = 3.15$ and $r = 3.6$, the first and fourth shows chaotic dynamics for $r = 3$ and $r = 3.8$. 28

4 Plot of K_c versus c for $R_r(x) = xe^{r(1-x)}$, 20000 data points and 1000 values of c were used, the parameter r varies as in the previous plots. The second and third picture shows regular dynamics for $r = 3.15$ and $r = 3.6$ - the values of K_c are mostly close to 0, while the first and fourth shows chaotic dynamics for $r = 3$ and $r = 3.8$ - K_c are close to 1. 29

5 Bifurcation diagram of $R_r(x) = xe^{r(1-x)}$. We used 20000 datapoints. 30

6 Plot of K versus r for $R_r(x) = xe^{r(1-x)}$ calculated with 20000 datapoints and 100 values of $c \in [\pi/5, 4\pi/5]$. For regular dynamics, K is close to 0, for chaotic dynamics K is close to 1. 30

7 Plot of the dependence of X_{n+1} (left) and X_{n+2} (right) on X_n of the function $F_\lambda(x) = \lambda x[1 - I(x)]$ for different values of the parameter λ. 34

8 Cobweb diagram of $F_\lambda(x) = \lambda x[1 - I(x)]$ for $\lambda = 1.7$ (on the left) and $\lambda = 2$ (on the right). The function is considered continuous for better visualisation. 35

9 Plot of p_c versus q_c for $F_\lambda(x) = \lambda x[1 - I(x)]$, for $r = 1.13$, $r = 1.34$, $r = 2.48$ and $r = 3.38$ on 10000 data points and 100 equally spaced values of c, $c \in [\pi/5, 4\pi/5]$. The first two pictures show regular dynamics by bounded trajectories in the (p, q)-plane, the third and fourth plot correspond to Brownian motion picturing chaotic dynamics. 35

10 Plot of K_c versus c for $F_\lambda(x) = \lambda x[1-I(x)]$. 10000 data points and 1000 values of c were used, the parameter λ varies as in the previous plots. The first two plots, for $\lambda = 1.13$ and $\lambda = 1.34$, show regular dynamics having values of K_c equal to 0, while the figures in the second row, for $\lambda = 2.48$ and $\lambda = 3.38$, display chaotic dynamics with values being closer to 1. 36

11 Bifurcation diagram of $F_\lambda(x) = \lambda x[1 - I(x)]$. We used 10000 data points. 37

12 Plot of K versus λ for $F_\lambda(x) = \lambda x[1-I(x)]$ calculated with 10000 data points and 100 values of $c \in [\pi/5, 4\pi/5]$. For regular dynamics, K is close to 0, for chaotic dynamics K is close to 1. 37

Listings

1 Code for the 0-1 test for chaos in Matlab. 21
2 Code for the bifurcation diagram in Matlab. 23
3 Code for the cobweb diagram in Matlab. 24
4 Plot of the Ricker model 10 in Matlab. 31
5 Code of the equation of the Ricker model 10 in Matlab. 31
6 Plot of the model for discrete and nonoverlapping generations regulated by microparasites 15 in Matlab. 38
7 Code for solving the implicit equation in Matlab. 38
8 Code of the equation of the model 15. 38

1 Introduction

Dynamical systems theory has a relatively short history and has drawn interest from many scientific fields over the years. The techniques used to study nonlinear dynamical systems can be applied to various problems from physics, chemistry, economics, biology, and ecology. Systems which were difficult to analyze can now be resolved in a geometric or qualitative solution. Chaos and random behavior are considered natural to the dynamical systems. In the next part the evolution of the chaos theory is briefly described.

Modern dynamical systems theory began when H. Poincaré [38] who studied the three-body problem and was the first to discover a chaotic deterministic system. He also introduced qualitative techniques for geometrical and topological problems.

A. Lyapunov [31] studied the behavior of points in the neighborhood of the equilibria, introducing the notion of Lyapunov stability. Later, while extending his study to any two infinitesimally close points, the notion of Lyapunov exponent was presented. This method for measuring the rate at which orbits of such points diverge is one of the key methods in studying and quantifying chaos.

Another important notion regarding dynamical systems, the ergodic theory, concerns the behavior of the system which is allowed to run for a long time. The greatest contribution in this field was done by two mathematicians. G. D. Birkhoff, who introduced a notion of transitivity for flows in [6]. Later on, the Birkhoff Ergodic Theorem was presented in [5]. J. von Neumann made foundational contributions to the ergodic theory in a series of articles [18] published around 1932, including the proof [44].

The first definition of chaos was set by T. Y. Li and J. A. Yorke [26]. According to them, a map is chaotic if there is an uncountably infinite set that is scrambled under the map, meaning that every two points in the set come infinitely close under some iteration of the map without staying close. The authors also proved that period three implies chaos for continuous self maps on an interval.

The Sharkovskii's theorem formulated by A. M. Sharkovskii states that if the continuous map has a periodic point of period three then it has periodic points of all other periods [8]. It only holds for maps of the real line and it is not possible to generalize it to all maps and spaces.

A new definition of chaos was brought by R. L. Devaney [8]. In his sense, the map is chaotic on a set if it has sensitive dependence on initial conditions, is topologically transitive, and the periodic points are dense in the set. It was later proved that the first assumption is unnecessary [2].

The notion of distributional chaos was introduced [42] after showing that the chaos in the sense of Devaney or Li and Yorke is not stable, meaning that some functions can lose the chaotic behavior under arbitrary small perturbations. Is is defined by a sequence of distribution functions of distance between the orbits equal to two points.

There are many other definitions of chaos, for example ω-chaos [25], Block-Coppel's chaos[20], Robinson's chaos[40] or Kato's chaos[16], whereas all contain unsolved implications[17, 22], so it can not be determined which one of them is the strongest.

1.1 Organization and goals of the thesis

This thesis focuses mainly on the 0-1 test for chaos introduced by Gottwald and Melbourne in [12].

Section 2 contains the basic definitions and notions that will be used later in the text.

After that, a short introduction to the 0-1 test for chaos is given in Section 3 together with an overview of the use of this test with examples from various scientific fields.

Different tools for chaos detection which are used in this thesis are presented in Section 4. The main goal is on the background of the 0-1 test for chaos (Subsection 4.1), but we will also take a look at bifurcation theory (Subsection 4.2), since the obtained results of the 0-1 test for chaos (see Figures 6 and 12) are compared with bifurcation diagrams (see Figures 5 and 11).

The implementation of the tests is described by using information for the test in the previous section. These are accompanied by direct codes in Matlab for other methods used in this thesis, for the bifurcation diagram, cobweb diagram, and plots of the models.

The implementations of the test are applied to two models from population biology in Section 6, where the first model given in Subsection 6.1 is in explicit form, while the second one, studied in Subsection 6.2, in implicit form. In both cases classical analysis of dynamical properties is performed or applied. The models are chosen from [34].

The goal of this thesis is to study typical maps of discrete dynamical systems by a new method - the 0-1 test for chaos. The test is implemented in Matlab and the numerical experiments are done on two models. These results are compared with bifurcation diagrams.

2 Preliminaries

The basic definitions and propositions from elementary dynamics are set in this section. Many of them belong in mathematical folklore and can be found in e.g. [8].

By a *discrete dynamical system* we mean an ordered pair

$$(X, f)$$

where X is the state space and $f : X \to X$ an onto (not necessarily into) action on X [23].

The map $f : X \to X$ is assumed to be continuous in this thesis. There are studied systems such that f is not continuous, e.g. some weak conditions are assumed, like connected G_δ graphs, see e.g. [47, 48]. The space X is standardly taken as a compact metric. Nevertheless, some generalizations or extensions are possible. In the Section 6 the space X is not compact, i.e. $X = [0, \infty)$, that is not restrictive, since this space is *f-invariant*, that is $f(X) \subseteq X$. Hence all iterations of any point from X remain in X.

The theory of (discrete) dynamical systems focuses on a behavior of state space point movement. That is represented as iterations:

$$f^n(x) = \underbrace{f \circ f ... \circ f}_{n-times}(x)$$

where f^n stands for the n-th iteration of the point x under the map f, here f^0 denotes the identity map on X.

The set $\mathrm{Orb}_f(x) = \{f^{n-1}(x) | n \in \mathbb{N}\}$, called an *orbit of x under the map f*.

Definition 1 *The point x is a fixed point for f if $f(x) = x$.*
The point x is a periodic point of period n if $f^n(x) = x$. The least positive n for which $f^n(x) = x$ is called the prime period of x.
We denote the set of periodic points of (not necessarilly prime) period n by $\mathrm{Per}_n(f)$, and the set of fixed points by $\mathrm{Fix}(f)$.
The set of all iterates of a periodic point form a periodic orbit.

Definition 2 *Let p be a periodic point of prime period n. The point p is hyperbolic if*

$$|(f^n)'(p)| \neq 1.$$

The number $(f^n)'(p)$ is called the multiplier of the periodic point.

Definition 3 *Let p be a hyperbolic periodic point of period n with $|(f^n)'(p)| < 1$. The point p is called an attracting periodic point (an attractor) or a sink.*

Definition 4 *A fixed point p with $|f'(p)| > 1$ is called a repelling fixed point (a repellor) or a source. The neighborhood described in the proposition 1 is called the local unstable set and denoted W^u_{loc}.*

The following statements will be useful tools used in Section 6.

Proposition 1 *Let p be a hyperbolic fixed point with $|f'(p)| < 1$. Then there is an open interval U about p such that if $x \in U$, then $\lim_{n\to\infty} f^n(x) = p$.*

Proposition 2 *Let p be a hyperbolic fixed point with $|f'(p)| > 1$. Then there is an open interval U about p such that if $x \in U$, $x \neq p$, then there exists $k > 0$ such that $f^k(x) \notin U$.*

3 Overview of the 0-1 test for chaos

The 0-1 test for chaos is one of the methods for distinguishing between regular and chaotic dynamics of a deterministic system. In contrast to the other approaches, the nature of the system is irrelevant, so the test can be applied directly onto experimental data, ordinary differential equations, or partial differential equations. The results obtained are close to 0 or 1, 0 corresponding to regular dynamics and 1 to chaotic dynamics. With its easy implementation, evaluation, and wide range of application, using this tool for detecting chaos is becoming more popular in different fields. In the next section, we offer a few recent examples of the 0-1 test being used on experimental data, as well as on discrete or continuous time systems.

3.1 Application on experimental data

The 0-1 test for chaos can be used directly on the data, which is what makes it a favourite tool to use with data obtained experimentally.

In [9] the 0-1 test for chaos is used along with the phase space reconstruction method to study the combustion process in the premixed natural gas engine. The data are obtained under different injection timing conditions. The results show that, under different conditions, the combustion process is chaotic.

A similar problem is discussed in [10] where the real-time series is experimentally obtained through a piezoelectric transducer. The data of in-cylinder pressure during the combustion process are analyzed by the 0-1 test, the largest Lyapunov exponent and the phase space reconstruction method. As the results of the 0-1 test K_c were equal to 1, the largest Lyapunov exponents were positive, and the attractors were limited to the finite range of phase space and had a twist and folded geometry structure, all the tests indicated chaotic behavior. It was also possible to observe the complexity and sensitivity on initial conditions of the combustion process.

Other example of using 0-1 test on experimental data is in [43] where the response of a piezoelectric material attached to a bistable laminate plate in a broadband piezoelectric based energy harvesting system is analyzed. The system is examined based on an experimentally generated voltage time series and it exhibited both periodic and chaotic behavior. To identify this, the frequency spectrum, bifurcation diagrams and phase portraits were also examined.

Another study of a vibrational energy harvester is shown in [28]. It is composed of a tip mass and a vertical beam which is excited and the vibrational energy is converted to electrical power. The tip mass is changed during the experiment. Bifurcations were observed from single well oscillations, along with regular and chaotic vibrations between the potential wells. The appearance of chaotic dynamics is shown by the bifurcation diagram, Fourier spectra, phase portraits and confirmed by the 0-1 test.

A similar example is [19] where a vibrational energy harvester with a bistable beam is studied to identify the vibration modes and the levels of power in each dynamic mode. During the

subjuction to harmonic excitations, the system exhibited both periodic and chaotic vibrations. The chaotic behavior is identified by return maps, multiscale entropy and the 0-1 test.

An interesting use of the test is seen in [21] where solar irradiance data is investigated by 0-1 test as well as by correlation dimension analysis, information entropy, recurrence plot and recurrence quantification analysis. However, chaotic behavior was not confirmed. The studied experimental data were collected from the Earth Radiation Budget Satellite during the period of 19 years.

In [32] data of traffic speed are studied by the 0-1 test for chaos, Lyapunov exponents and the notion of Shannon entropy. The noise was diminished by wavelet shrinkage and the dynamical properties are estimated by the 0-1 test, which indicated strong chaos. The values of the maximal Lyapunov exponent and Shannon entropy are related to the predictability of the system and changes in dynamics on different time scales.

In [11] the 0-1 test for chaos is compared to other chaos detection methods, like Lyapunov exponent, conditional entropy of ordinal patterns and permutation largest slope entropy algorithm. The Duffing oscillator and its equivalent electronic circuit was used to generate the data. The experiment was done using a digital oscilloscope. Although, it concludes that the 0-1 test worked better with the simulated data then with the experimental data.

3.2 Application on discrete dynamical systems

The 0-1 test is also popular with data modeled by equations describing discrete dynamical systems. Studying a third-order autonomous memristive chaotic oscillator in [3] led to identifying periodic, quasi-periodic and chaotic dynamics using different methods. Beginning by modeling the oscillator, stability analyzes, numerical simulations, time-domain sequence, bifurcation diagram and Lyapunov exponents were calculated. The paper focuses on quasi-periodic behavior and point-cycle chaotic bursting which were identified by the 0-1 test. The results are confirmed by hardware experiments.

In [41] shape memory alloy dynamical systems are analyzed focusing on the application of 0-1 test. The study included various constitutive models for the restitution force on single- and two-degree of freedom oscillators. The results are compared with Lyapunov exponents calculated with different algorithms and the 0-1 test for chaos is considered a reliable and efficient tool for chaos detection.

Another example of using the 0-1 test for chaos is in [30]. The Melnikov method was used to find the necessary conditions for chaos - increase of noise intensity. The amplitude of randomly disordered periodic was determined by calculating the largest Lyapunov exponent, which was also used along with phase portraits and Poincaré maps to confirm the effects of noise intensity on chaotic behavior of the piezoelectric vibration energy harvester system. The 0-1 test for was used particularly to quantify the responses of the vibration energy harvester.

In [46] the 0-1 test is used to demonstrate chaotic dynamics in a fractional-order switched system. A fractional-order unstable dissipative system is proposed whose chaotic behavior is

found with a specific fractional order. Transformed to an equivalent switched system with augmented states, it is implemented on an ARM system on-chip board. This study combines both simulated and experimental data, and the 0-1 test is used along with a chaos definition for finite state sets to demonstrate chaotic dynamics.

Another example with a vibrational energy harvester is [7]. It is shown that the fractional order of damping considerably affects the power output.The dynamic responses are examined using phase trajectory, Fourier spectrum, multiscale entropy and 0-1 test. The results show that the system exhibits both periodic and chaotic motion based on fractional order changes.

3.3 Application on continuous dynamical systems

Although the use of the 0-1 test for chaos is more popular with discrete time systems, we can mention [35], where the authors discuss some features of the 0-1 test, like resonance and oversampling, while demonstrating their results for typical chaotic systems such as memristive circuits.

Another example is the use of the test to monitor chaotic bit generators in [36]. It shows the chaotic nature of the continuous time signals and proves that it is inherited by the bit sequence even when using a simple threshold comparator. The results are simulated by the Chua and Lindberg-Murali-Tamasevicius circuits.

In [24], a mechanical system of a jumping ball is studied regarding dynamic properties. After considering all the mechanical properties of the system, the motion of the ball is described by a set of two nonlinear ordinary differential equations solved by the Runge-Kutta method. It is shown by the 0-1 test, bifurcation diagram and Fourier spectra, that the system exhibits regular, irregular and chaotic behavior for different choices of parameters.

A cutting process is analyzed in [29] using a two degree of freedom non-smooth model with a friction component in order to identify chaotic motion. The maximum Lyapunov exponent was proved to be unreliable due to the non-smoothness of the model. The 0-1 test for chaos, on the other hand, is not limited regarding smoothness, so it is a good method to study the dynamic of this system, which is useful in machining technology to improve vibration control and design relevant system parameters.

Another example is [27] where thermomechanical shape memory oscillators are studied. The 0-1 test is used to reveal the chaotic nature of trajectories in case of neglected temperature variations. The results were confirmed by the Fourier spectra. Different levels of chaoticity were analyzed comparing their qualitative difference to different values of the parameter K.

4 Tools of dynamics detection

As we have seen in Section 3, many tools and their combinations are used to investigate dynamics of a system. This thesis is focused on the 0-1 test for chaos, but the results are compared to bifurcation diagrams, therefore these two methods are also briefly described in the section that follows.

4.1 The 0-1 test for chaos

The 0-1 test is a useful tool for evaluating dynamics in deterministic systems. In this section we discuss the test and its implementation in more detail.

The idea for the 0-1 test is based on the study of two-dimensional Euclidian extension [4]. The degrees of freedom introduced by the extension are represented by three scalars (p, q, ϑ), where p, q are the coordinates of the position in the plane and ϑ is the angle of rotation of the virtual point. In [12] they are defined by iterating the extended system as:

$$\begin{cases} p_c(n+1) = p_c(n) + \phi(n)\cos(\vartheta(n)), \\ q_c(n+1) = q_c(n) + \phi(n)\sin(\vartheta(n)), \\ \vartheta_c(n+1) = \vartheta_c(n) + c + \alpha\phi(n). \end{cases}$$

Later in [14], the version for $\alpha = 0$ is found which is used in the implementation of the test. Given the observation $\phi(j)$ for $j = 1, 2, ..., N$:

$$p_c(n) = \sum_{j=1}^{n} \phi(j)\cos jc, \tag{1}$$

$$q_c(n) = \sum_{j=1}^{n} \phi(j)\sin jc \tag{2}$$

for $n = 1, 2, ..., N$.

As it is described in [4], periodic and quasi-periodic motion cause a bounded auxiliary trajectory in the (p, q) plane, whereas chaotic dynamics produce, under wide range of definitions of chaos [13, 14, 37], an unbounded trajectory. Thus using the 0-1 test to detect chaos is related to the ability to detect unbounded motion in the (p, q) plane. Along with this unboundedness, it tends to exhibit an irregular behavior similar to the Brownian motion, for which the probability distribution of the position of a particle at time t is Gaussian. As the Brownian motion is an ergodic process, we get the variance of this distribution as the time-averaged mean-square displacement of any specific trajectory evaluated over some time lag.

The idea for the 0-1 test, first described in [12] says that the boundedness or unboundedness of the trajectory $\{(p_j, q_j)_{j\in[1,N]}\}$ can be studied through the asymptotic growth rate of its time-

averaged mean square displacement, which is defined as

$$M(n) = \lim_{N\to\infty} \frac{1}{N} \sum_{j=1}^{N} d(j;n)^2 \tag{3}$$

where

$$d(j;n) = \sqrt{(p_{j+n} - p_j)^2 + (q_{j+n} - q_j)^2} \tag{4}$$

is the time lapse of the duration n ($n \ll N$) starting from the position at time j. As it is shown in [14, 15], it is important to use values of n small enough compared to N, noted $n_{cut}, (n \leq n_{cut})$. A subset of time lags $n_{cut} \in [1, N/10]$ is advised for the computation of each K_c.

$M(n)$ is the average of the displacements which can be different depending on the part of the trajectory. It is evaluated over all time lags.

If the time lag is fixed, the mean square displacement describes only the local behavior of the trajectory. In order to determine the overall unboundedness, larger values of n must be studied.

For bounded trajectories and regular dynamics $M(n)$ is a bounded function in time, whereas unbounded trajectories, meaning chaotic dynamics, are described by $M(n)$ growing linearly with time. Thus we must calculate the asymptotic growth rate of the MSD which correlates with the unboundedness of the trajectory.

When first proposed in [12], the asymptotic growth rate was defined as the average logarithmic growth rate of the MSD

$$K_c = \lim_{n\to\infty} \frac{\log M(n)}{\log n}. \tag{5}$$

In the following paper [14] the authors propose a modified MSD, which is defined as

$$D(n) = M(n) - E(\phi)^2 \frac{1 - \cos nc}{1 - \cos c} \tag{6}$$

along with a new correlation method for computing the asymptotic growth rate

$$K_c = \lim_{n\to\infty} \frac{\mathrm{cov}(x, D)}{\sqrt{\mathrm{var}(x)\mathrm{var}(D)}} \tag{7}$$

which have been proved to give better results than the regression method (5).

It is shown in [37] that the dynamics of the extension is sublinear in case of chaos, which results in K_c equal either 0 for regular dynamics, or 1 for chaotic behavior of the trajectory. K_c is dependent on the parameter c, which also has an important role in the computations. K_c is calculated for all the values of c, then the final indicator K is equal to the median of these results.

The parameter c determines the studied extension and has a strong effect on the dynamics. There are exceptional values of c for which the parameter K_c may give false results, because of the resonance between the base dynamics and its group extension. For this reason K_c is computed for different, usually at least 100, values of c. As it was already mentioned, the final

result is

$$K = \text{median}(K_c).$$

The difficulties with calculating the limits entering the definition of K_c - the length of the signal $N \to \infty$, appearing in the definition of MSD, and the time lag $n \to \infty$ in the definition of K_c, do not practically pose a problem, as they are evaluated on time series of finite duration.

4.2 Bifurcation diagram

The bifurcation theory is built around bifurcations, which mean a division in two, a splitting apart, or a change. Its goal is to study the changes that maps undergo depending on changes in parameters, usually regarding changes involving the periodic point structure [8]. There are global bifurcations which are related to larger invariant sets, and local bifurcations which can be studied in a small neighborhood. Many types of local bifurcation exist, like for example saddle-node bifurcation, pitchfork bifurcation, period-doubling bifurcation or Hopf bifurcation [1]. The local bifurcation theory explains two usual ways how, with various values of the parameter, infinitely many periodic points can arise. It happens via saddle-node (or tangent) bifurcation or period-doubling bifurcation, which is a typical route to chaos [8]. In the following practical Section 6, we are going to see the representation of this theory, which is the bifurcation diagram. It is the plot of the locations of fixed or periodic points in function of the parameter.

5 On implementation in Matlab

The following codes shows the implementation of the 0-1 test for chaos, the bifurcation diagram and the cobweb diagram.

The implementation of the 0-1 test for chaos, see Listing 1 is inspired by [14]. Each step in the computation is commented in the code (in green). The first version was done to calculate the iterations of the functions directly, which was changed because of the implicitly given function which had to be computed separately. Now, the function is loaded from the matrix XX, where every row corresponds to the iterations of the function for one value of the parameter.

```
function[] = testchaos(XX,N,mi1,mistep,mi2,c1,ccount,c2)
% XX          data matrix
% N           number of data points / number of iterations per parameter
% mi1         first value of the function parameter
% mistep      increment of the parameter
% mi2         last value of the parameter
% c1          first value of the parameter c
% ccount      number of parameters c used
% c2          last value of parameter c

% initialization
    ncut = N/10;
    x = zeros(N,1);
    y = zeros(N,1);
    z = zeros(N,1);
    pc = zeros(N,1);
    qc = zeros(N,1);
    mctemp = zeros(ncut,1);
    mc = zeros(ncut,1);
    vosc = zeros(ncut,1);
    dc = zeros(ncut,1);
    xi = zeros(ncut,1);
    delta = zeros(ncut,1);
    indexkc = 1;
    indexk = 1;
    indexmi = 1;

% main loop
    for mi = mi1:mistep:mi2
        x = XX(indexmi,:); % function
```

```
        for c = c1:(c2-c1)/ccount:c2
            for j = 1:1:N
                y(j) = x(j)*cos(j*c);
                z(j) = x(j)*sin(j*c);
                pc(j) = sum(y); % translation variable pc
                qc(j) = sum(z); % translation variable qc
            end
            E = (1/N)*sum(x);
            for n = 1:1:ncut
                for j = 1:1:ncut
                    mctemp(j) = ((pc(j+n)-pc(j))^2)+((qc(j+n)-qc(j))^2);
                end
                mc(n) = (1/ncut)*sum(mctemp); % mean square displacement
                vosc(n) = (E^2)*(1-cos(n*c))/(1-cos(c));
                dc(n) = mc(n) - vosc(n); % modified mean square displacement
            end
            for n = 1:1:ncut
                xi(n) = n;
                delta(n) = dc(n);
            end
            R = corrcoef(xi,delta); % correlation coefficient
            kc(indexkc) = R(1,2); % calculation of kc
            indexkc = indexkc+1;
        end
        indexkc = 1;
        k(indexk) = median(kc); % calculation of the control parameter k
        indexk = indexk+1;
        indexmi = indexmi+1;
    end

% plot
    vectormi = mi1:mistep:mi2;
    scatter(vectormi,k,10,'.') %scatter plot of k versus the parameter mi
end
```

Listing 1: Code for the 0-1 test for chaos in Matlab.

The following code for the bifurcation diagram, see Listings 2, is based on [45]. The first 500 points on the orbit are omitted in the plot in order to eliminate the early transient behavior. Each loop represents one iteration and corresponds to one surface plot. In the end the view

on all the $N - 500$ surfaces is rotated around the z axis to accommodate only the y and z axis corresponding to the parameter of the function and the values visited respectively. The final bifurcation diagram is obtained as the intersection of the surfaces.

```
function mat = bifurMat(XX,mi1,mi2,N)

% XX    data matrix
% mi1   the start value of parameter a
% mi2   the end value of parameter a
% N     the number of iterations of the function

% initialization
[inr,inc] = size(XX);
mat = zeros(inr,N);
mi = linspace(mi1,mi2,inr);

% main loop
format long
for i = 1:inr
    ix = 1;
    ca = i; % pick one parameter value at each time
    for j = 1:N % generate a sequence with length L
        if j == 1
            pre = ix; % assign initial value
            for k = 1:500 % throw out bad data
               nxt = XX(ca,pre);
               ix = ix +1;
               pre = ix;
            end
        end
        nxt = XX(ca,pre); % generate sequence
        mat(i,j) = nxt; % store in mat
        ix = ix + 1;
        pre = ix; % use latest value as the initial value for the next round
    end
end

% plot
dcolor = [0,0.45,0.74];
[r,c] = meshgrid(1:N,mi); % associated coordinate data
```

```
surf(r,c,mat,'Marker','.','MarkerSize',1,'FaceColor','None','MarkerEdgeColor',
    dcolor,'EdgeColor','None')
view([90,0,0]) % change camera direction
ylim([mi1,mi2]) % fit to data
```

Listing 2: Code for the bifurcation diagram in Matlab.

The creation of the cobweb plot is shown on Listing 3. The entering functions are shown on Listings 5 and 8.

```
function cobweb(f,x1,x2,mi,N)

% f     function, as e.g. model1R or model2F
% x1    beginning of the interval on which we plot the function
%       also the initial value of x, x1>0
% x2    end of the interval on which we plot the function
% mi    parameter of the function
% N     number of values in the interval

y=zeros(N,1);
x=linspace(x1,x2,N);

for i=1:N
    y(i)=f(x(i),mi);
end
hold on;
plot(x,y,'Color',[0 0.45 0.74]); %plot of the function
plot(x,x,'k'); %plot of the diagonal
for i=1:N
    x(i+1)=f(x(i),mi);
    line([x(i),x(i)],[x(i),x(i+1)],'Color',[0.85 0.33 0.1]);
    line([x(i),x(i+1)],[x(i+1),x(i+1)],'Color',[0.85 0.33 0.1]);
end
hold off;
```

Listing 3: Code for the cobweb diagram in Matlab.

6 Application of the test

The implemented test was applied on two models chosen from [34]. The first one (10) is given in explicit form, while the second one (15) in implicit form.

6.1 Ricker model

The model is inspired by studies of fish population and reproduction in [39]. This classic discrete population model describes the expected density of individuals N_{t+1} in the next generation as a function of individuals in the previous generation N_t.

The relation is given by the equation

$$N_{t+1} = N_t e^{r(1-N_t/N_T)} \tag{8}$$

where r is an intrinsic growth rate and N_T is the carrying capacity of the environment. As the variable N_T enters the equation only to set the scale of N, we replace it by a dimensionless variable

$$Y = N/N_T$$

Hence, we obtain the equation

$$Y_{t+1} = Y_t e^{r(1-Y_t)} \tag{9}$$

Let (X, R_r) be a discrete dynamical system where $X = [0, \infty)$ and the map $R_r : X \to X$ defined by

$$R_r(x) = xe^{r(1-x)}. \tag{10}$$

If $r = 0$ the system (10) degenerates into the trivial case of identity, hence for the next calculations the parameter r will be assumed to be non zero.

Theorem 1 *Let (X, R_r) be a discrete dynamical system (10) with $r \neq 0$. Then* $\mathrm{Fix}\,(R_r) = \{0, 1\}$.

Proof

For the proof it is necessary to solve the equation

$$R_r(x) = x$$

that is

$$x = xe^{r(1-x)}.$$

Omitting the trivial solution $x_0 = 0$ *we solve the equation*

$$1 = e^{r(1-x)}$$

that yields

$$x_1 = 1.$$

Consequently $\mathrm{Fix}\,(R_r) = \{0, 1\}$*, ending the proof.* ∎

The map and its second iteration are depicted on Figure 1 for different values of a positive parameter r. The fixed point $x_1 = 1$ does not depend on the parameter and can be identified as the intersection of the graph of R_r with the diagonal i.e. $R_r(x) = x$. The implementation of the plot in Matlab is shown on Listing 4.

On Figure 2 the first cobweb diagram for $r = 1.5$ shows an inward spiral converging to the fixed point $x_1 = 1$. The other diagram for $r = 2.5$ depicts an outward spiral ending in a rectangular shape detecting a period 2 orbit. The creation of the cobweb diagram in Matlab is shown on Listing 3 while the implementation of the function called, corresponding to (15), is on Listing 5.

Theorem 2 *Let* (X, R_r) *be a discrete dynamical system defined by* (10)*. Then*

1. *if* $r > 0$ *then the fixed point* $x_0 = 0$ *is a repelor,*
2. *if* $r < 0$ *then the fixed point* $x_0 = 0$ *is an attractor.*

Proof
By direct calculations one gets

$$R_r'(x) = e^{r(1-x)}(1 - rx). \tag{11}$$

For $r > 0$ *it is* $|R_r'(x_0)| > 1$*, hence using Proposition 2* x_0 *is a repelor.*
On the other hand if $r < 0$ *it is* $|R_r'(x_0)| < 1$*, hence using Proposition 1* x_0 *is an attractor, ending the proof.* ∎

Theorem 3 *Let* (X, R_r) *be a discrete dynamical system defined by* (10)*. Then*

1. *if* $r > 0$ *then the fixed point* $x_1 = 1$ *is an attractor,*
2. *if* $r < 0$ *then the fixed point* $x_1 = 1$ *is a repelor*

Proof
Analogically, using (11) *for* $r > 0$ *it is* $|R_r'(x_1)| < 1$*, hence by Proposition 1* x_1 *is an attractor.*
On the other hand if $r < 0$ *it is* $|R_r'(x_1)| > 1$*, hence applying Proposition 2* x_1 *is a repelor, ending the proof.* ∎

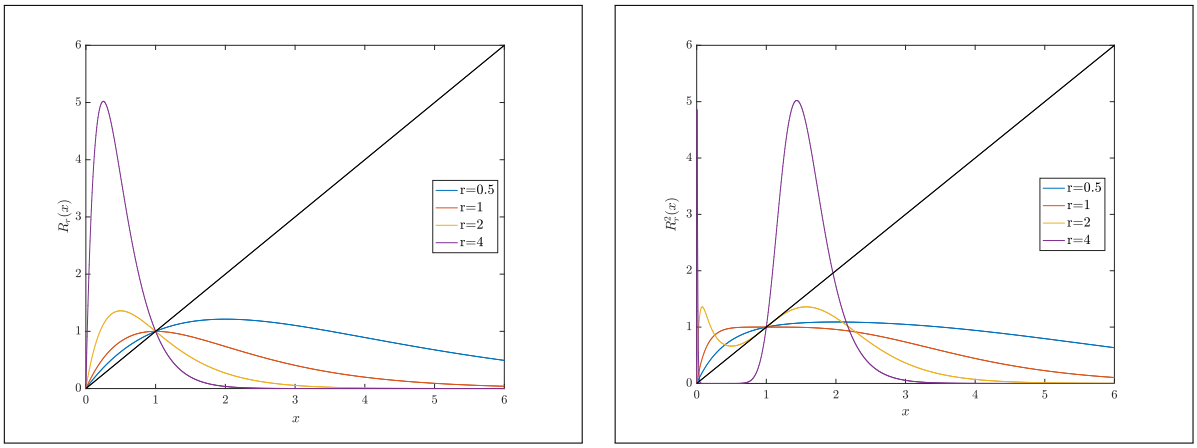

Figure 1: Plot of first (on the left) and second (on the right) iteration of the function $R_r(x) = xe^{r(1-x)}$ for different values of the parameter r.

The investigation of the dynamics of the system (10) is shown on the next figures. The simulations were performed for orbits that were calculated in Matlab for the initial value $x_0 = \sqrt{2}/2$. In this case 20000 iterations were computed for each parameter r in the range for 2 to 4 by 0.01. The outputs of the test are shown and described in the following.

Figure 5 represents the bifurcation diagram which shows the values visited as a function of the parameter r ranging from 2 to 4. The points in which the forking occurs are period-doubling bifurcations. The dark stripes visualize chaos while the light parts, where periodic orbits are visible, represent regular dynamics.

The following figures are related to the outputs of the 0-1 test for chaos.

Figure 3 shows how $p_c(n)$ and $q_c(n)$ are bounded if the underlying dynamics are regular. This can be seen in the second and third picture (for $r = 3.15$ and $r = 3.6$) with a symmetric shape. On the other hand, the first and fourth picture ($r = 3$ and $r = 3.8$) depicts a Brownian motion which is characteristic for chaotic dynamics.

In Figure 4 the control parameter of the 0-1 test K_c is plotted versus c ranging from π to 2π for four values of r chosen as in the previous Figure 3. The second and third picture corresponding to regular dynamics show values of K_c close to 0, except for a few isolated values of c due to resonance. The first and fourth plot show chaotic dynamics, as the values of K_c are close to 1. In this case the values of K_c are more diverse, nevertheless the majority is close to 1, and the final control parameter K of the test is calculated as the median of these values.

The final result of the test is shown on Figure 6 as the value of K as a function of the parameter r ranging from 2 to 4 by 0.01. The test was calculated for 100 equally spaced values of $c \in [\pi/5, 4\pi/5]$ and for $N = 20000$. The values of K close to 0 correspond to regular dynamics, values close to 1 to chaotic dynamics. It is possible to confirm that the test corresponds with the bifurcation diagram precisely, although we can also observe a few values that are neither 0 nor 1.

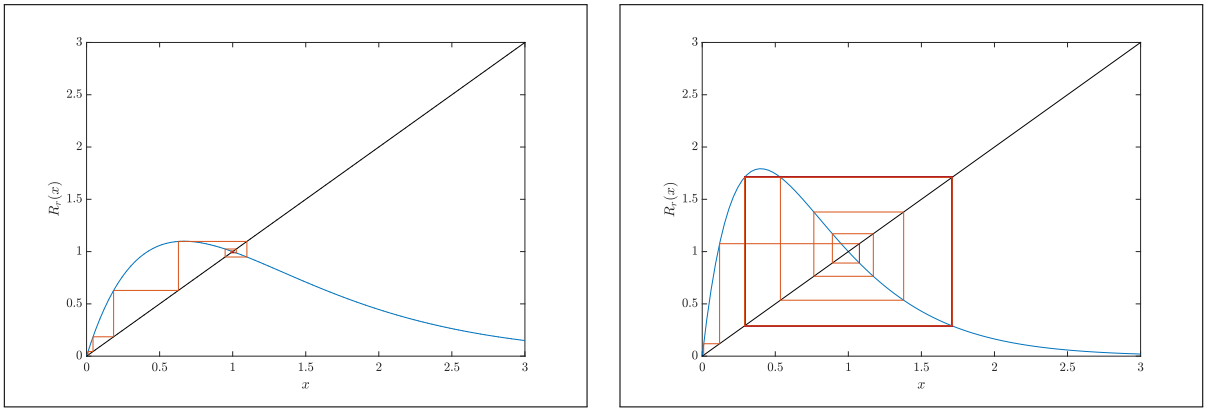

Figure 2: Cobweb diagram of $R_r(x) = xe^{r(1-x)}$ for $r = 1.5$ (on the left) and $r = 2.5$ (on the right). It shows the fixed point $x_1 = 1$.

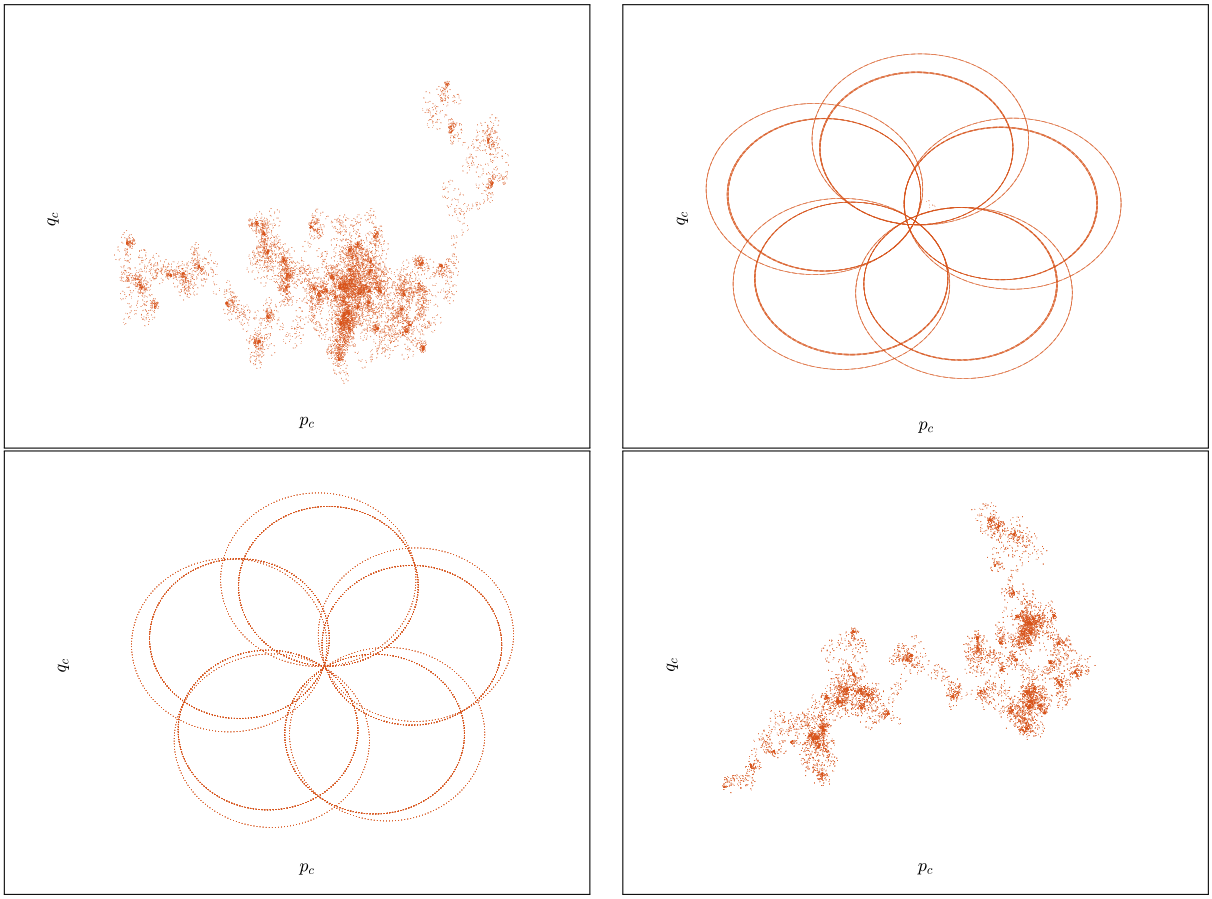

Figure 3: Plot of p versus q for $R_r(x) = xe^{r(1-x)}$, for $r = 3$, $r = 3.15$, $r = 3.6$ and $r = 3.8$ on 20000 data points and 100 equally spaced values of c, $c \in [\pi/5, 4\pi/5]$. The second and third picture shows regular dynamics for $r = 3.15$ and $r = 3.6$, the first and fourth shows chaotic dynamics for $r = 3$ and $r = 3.8$.

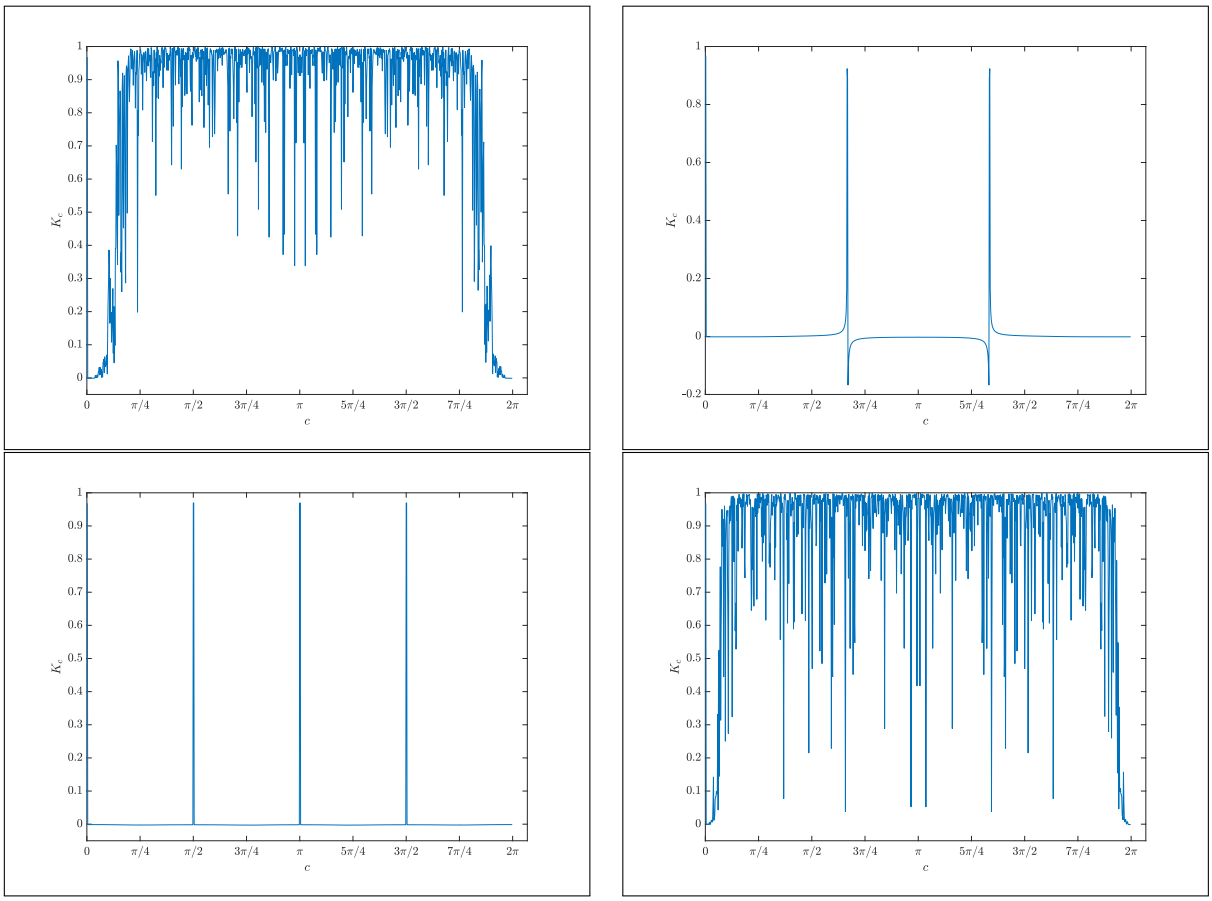

Figure 4: Plot of K_c versus c for $R_r(x) = xe^{r(1-x)}$, 20000 data points and 1000 values of c were used, the parameter r varies as in the previous plots. The second and third picture shows regular dynamics for $r = 3.15$ and $r = 3.6$ - the values of K_c are mostly close to 0, while the first and fourth shows chaotic dynamics for $r = 3$ and $r = 3.8$ - K_c are close to 1.

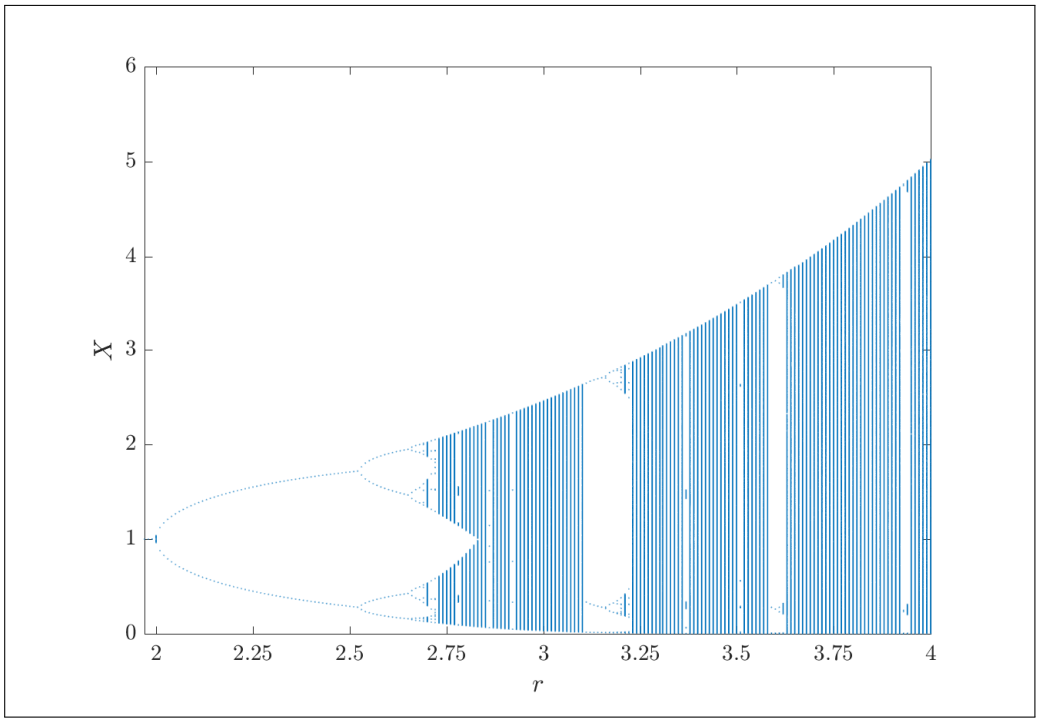

Figure 5: Bifurcation diagram of $R_r(x) = xe^{r(1-x)}$. We used 20000 datapoints.

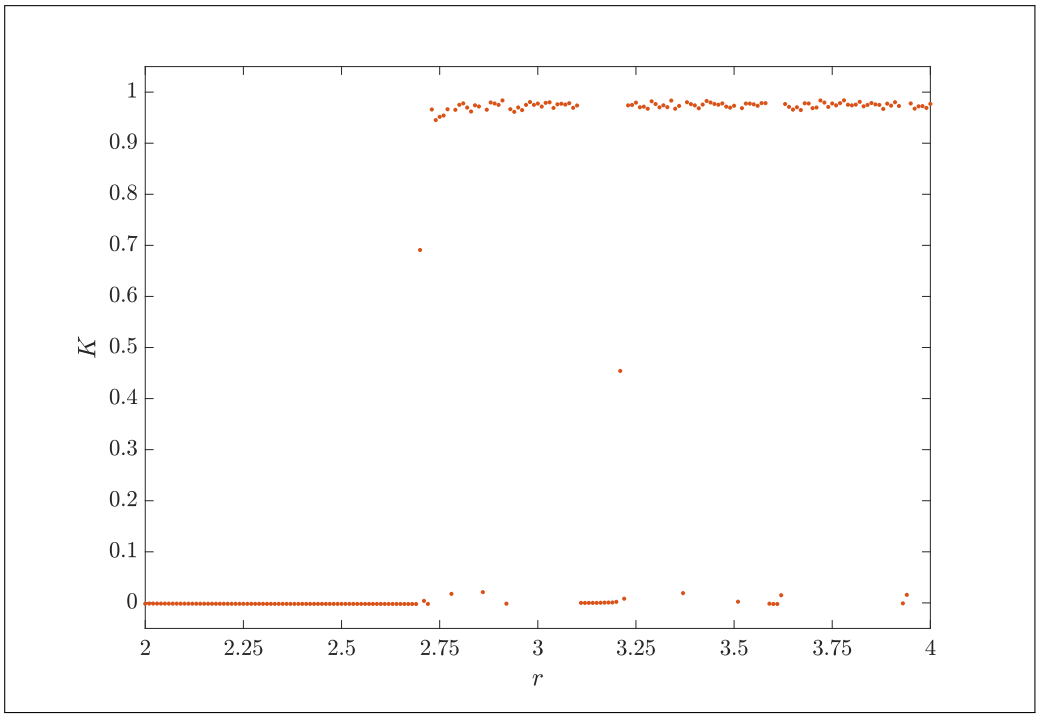

Figure 6: Plot of K versus r for $R_r(x) = xe^{r(1-x)}$ calculated with 20000 datapoints and 100 values of $c \in [\pi/5, 4\pi/5]$. For regular dynamics, K is close to 0, for chaotic dynamics K is close to 1.

```
function model1plot(r,x1,x2,N)

% r     parameter of the function
% x1    beginning of the interval on which we plot the function
% x2    end of the interval on which we plot the function
% N     number of values in the interval

    x = linspace(x1,x2,N);
    y = x.*exp(r.*(1-x));
    plot(x,y);
end
```

Listing 4: Plot of the Ricker model 10 in Matlab.

```
function[y] = model1R(x,r)
   y= x.*exp(r.*(1-x));
end
```

Listing 5: Code of the equation of the Ricker model 10 in Matlab.

6.2 Discrete and nonoverlapping generations regulated by microparasites

As it is described in [33] the model is based on populations with discrete, nonoverlapping generations that have their density regulated by parasitoids - viral, bacterial or protozoan microparasites.

In the studied model for density-dependent regulation of a host population with nonoverlapping generations by a microparasite, the pathogen is assumed to spread through each generation. The fraction of the host population that has been infected I, is related to the magnitude of the population N and is modeled by the equation

$$1 - I = e^{-IN/N_T}, \tag{12}$$

N_T is described as a threshold host density.

If $N < N_T$ the reproductive rate of the parasitoid is less than 1 and the epidemic cannot be established. The solution of the equation (12) is $I = 0$.
If $N > N_T$ the epidemic spreads and there exists a nontrivial solution to the equation (12) where $I \neq 0$.

We assume that the pathogen is lethal and it runs its course before reproduction. Thus the fraction of the population which survived and is able to reproduce is

$$N_{t+1} = \lambda N_t[1 - I(N_t)] \tag{13}$$

where I is given by the equation 12.

The equation 13 describes such a population in generation $t + 1$ with the host population of magnitude N_t and an intrinsic per capita reproductive rate λ. As the variable N_T enters the equation only to set the scale of N, we replace it by a dimensionless variable

$$Y = N/N_T$$

Hence, we obtain the equation

$$Y_{t+1} = \lambda Y_t[1 - I(Y_t)] \tag{14}$$

Let (X, F_λ) be a discrete dynamical system where $X = [0, \infty)$ and the map $F_\lambda : X \to X$ defined by

$$F_\lambda(x) = \lambda x[1 - I(x)] \tag{15}$$

where $I(x)$:

$$1 - I = e^{-Ix} \tag{16}$$

Theorem 4 *Let* (X, F_λ) *be a discrete dynamical system* (15) *with* $\lambda > 1$. *Then* $\mathrm{Fix}\,(F_\lambda) = \{0, \lambda \ln \lambda/(\lambda - 1)\}$.

Proof
For the proof it is necessary to solve the equation

$$F_\lambda(x) = x$$

that is

$$x_\lambda = \lambda x[1 - I(x)].$$

Omitting the trivial solution $x_0 = 0$ *we solve the equation*

$$1 = \lambda x[1 - I(x)]$$

that yields

$$x_1 = \frac{\lambda \ln \lambda}{\lambda - 1}.$$

Consequently $\mathrm{Fix}\,(F_\lambda) = \{0, \lambda \ln \lambda/(\lambda - 1)\}$, *ending the proof.* ■

The map and its second iteration are shown on Figure 7 for different values of parameter λ. This time the fixed point $x_1 = \lambda \ln \lambda/(\lambda - 1)$ depends on the parameter. This is obvious as the intersection of the plot with the diagonal $F_\lambda(x) = x$ varies as the parameter changes. The implementation of this plot in Matlab is shown on Listing 6.

On Figure 8 the first cobweb diagram for $\lambda = 1.7$ shows an outward spiral corresponding to an unstable fixed point. The same phenomenon is shown on the second cobweb diagram for $\lambda = 2$, which suggests that the system does not have any stable points. The code for the cobweb diagram in Matlab is shown on Listing 3 while the function called, corresponding to (15), is shown on Listing 8.

In case of this implicit function we omit further investigation of the attractivity of the fixed points as it is beyond the scope of this thesis and can be read in [33].

The experimental study of the dynamics was done in Matlab by calculating the orbits for the initial value $x_0 = \sqrt{2}/2$. The calculations were done for on 10000 iterations for each parameter λ only as the computations for this implicitly implemented function took longer and had to be done separately. We had 101 equally spaced values of λ ranging from 1.01 to 4.01. Compared to the study of the first model, it is obvious that the results are less precise. The outputs of the tests are discussed in the following.

Figure 11 represents the bifurcation diagram which shows the values visited as a function of the parameter λ ranging from 1.01 to 4.01 by 0.03. The values of X alternate between a band of high and low values. For small values of λ close to 1, it is possible to distinguish 4 narrow bands which could correspond to a period 4 orbit, merging into 2 wider bands around $\lambda = 1.7$.

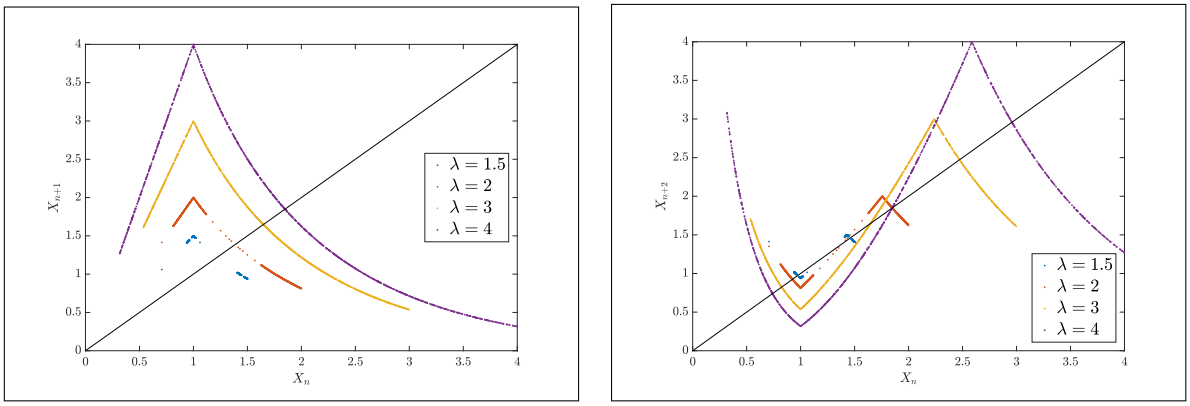

Figure 7: Plot of the dependence of X_{n+1} (left) and X_{n+2} (right) on X_n of the function $F_\lambda(x) = \lambda x[1 - I(x)]$ for different values of the parameter λ.

By λ reaching the value around 2.9 the two bands merge into one, which means X can reach any value from the band.

The following figures are related to the outputs of the 0-1 test for chaos.

Figure 9 shows the boundedness of the trajectories in the (p, q)-plane as the dynamics are regular. This can be seen in the first and the second figure. It is possible to note that the points on the second plot are less ordered, although we can still see the symmetrical shape, which correspond to the change from regular to chaotic dynamics. The third and fourth picture shows the typical Brownian motion characteristic for chaos.

In Figure 10 the control parameter of the 0-1 test K_c is plotted as a function of 1000 values of c ranging from π to 2π for four values of λ like in the previous Figure 9. The first two figures show K_c equal to 0 apart from a few points where resonance occurred, which corresponds to regular dynamics. The other two figures in the second row clearly depicts chaotic dynamics as the values of K_c are more variable, but they are mostly close to 1.

The result of the 0-1 test for chaos is shown in Figure 12 as the value of K as a function of the parameter λ ranging from 1.01 to 4.01 by 0.03. The test was again calculated for 100 values of c, $c \in [\pi/5, 4\pi/5]$, and for $N = 10000$. We notice that there are many points between λ equal to 1.5 and 2 that are not close to either 0 or 1. This may be caused by the small sample and could have been avoided by calculating more iterations. Based on the test only we could not conclude whether the dynamics of the system for the parameter $\lambda \in [1.5, 2]$ is regular or chaotic. Nevertheless, by comparing results of the 0-1 test for chaos in Figure 12 we can conclude that around $\lambda = 2$ the regular dynamics start turning into chaos which is related to the output of the bifurcation diagram in Figure 11.

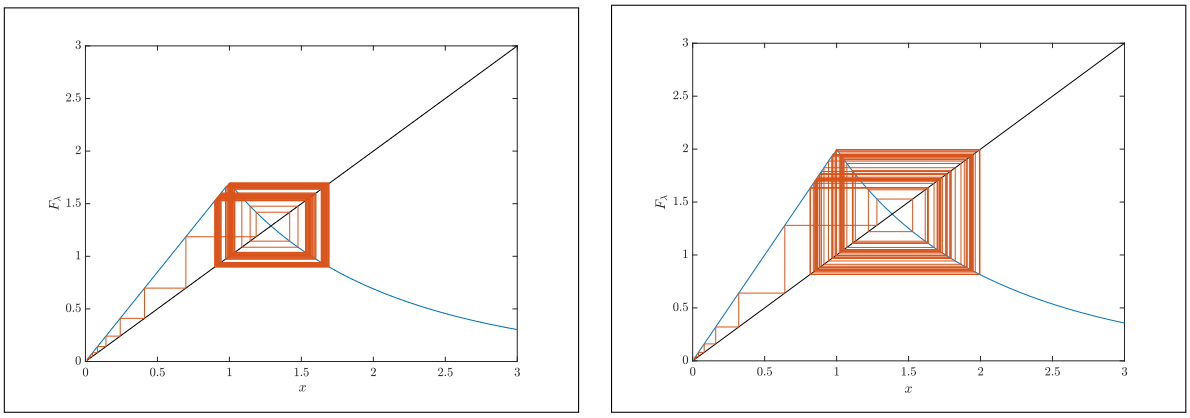

Figure 8: Cobweb diagram of $F_\lambda(x) = \lambda x[1 - I(x)]$ for $\lambda = 1.7$ (on the left) and $\lambda = 2$ (on the right). The function is considered continuous for better visualisation.

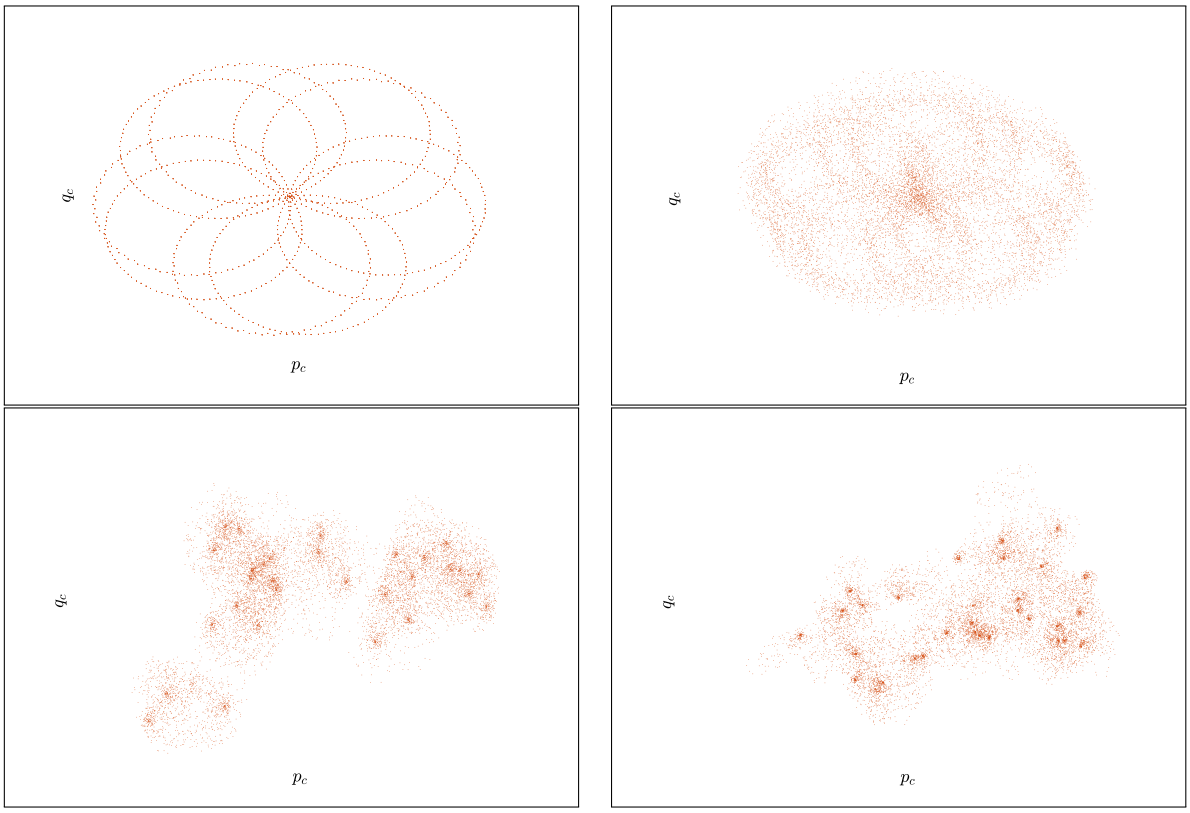

Figure 9: Plot of p_c versus q_c for $F_\lambda(x) = \lambda x[1 - I(x)]$, for $r = 1.13$, $r = 1.34$, $r = 2.48$ and $r = 3.38$ on 10000 data points and 100 equally spaced values of c, $c \in [\pi/5, 4\pi/5]$. The first two pictures show regular dynamics by bounded trajectories in the (p, q)-plane, the third and fourth plot correspond to Brownian motion picturing chaotic dynamics.

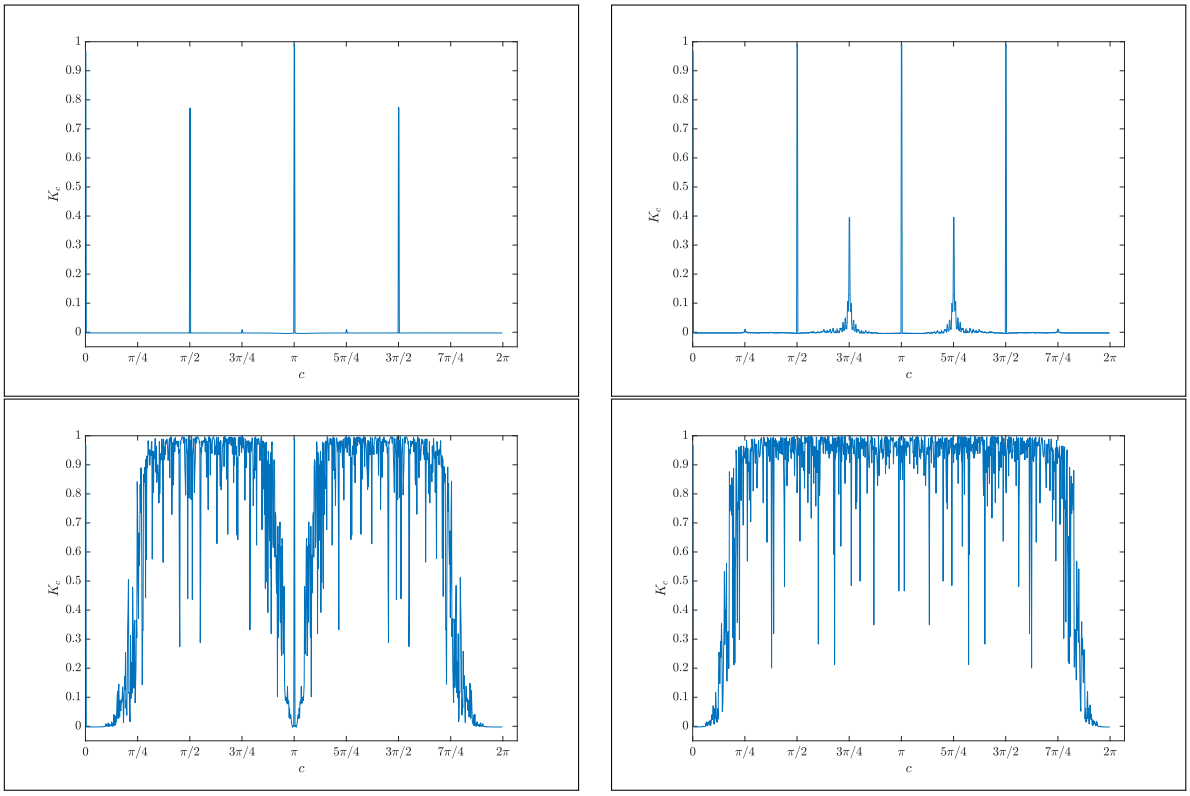

Figure 10: Plot of K_c versus c for $F_\lambda(x) = \lambda x[1 - I(x)]$. 10000 data points and 1000 values of c were used, the parameter λ varies as in the previous plots. The first two plots, for $\lambda = 1.13$ and $\lambda = 1.34$, show regular dynamics having values of K_c equal to 0, while the figures in the second row, for $\lambda = 2.48$ and $\lambda = 3.38$, display chaotic dynamics with values being closer to 1.

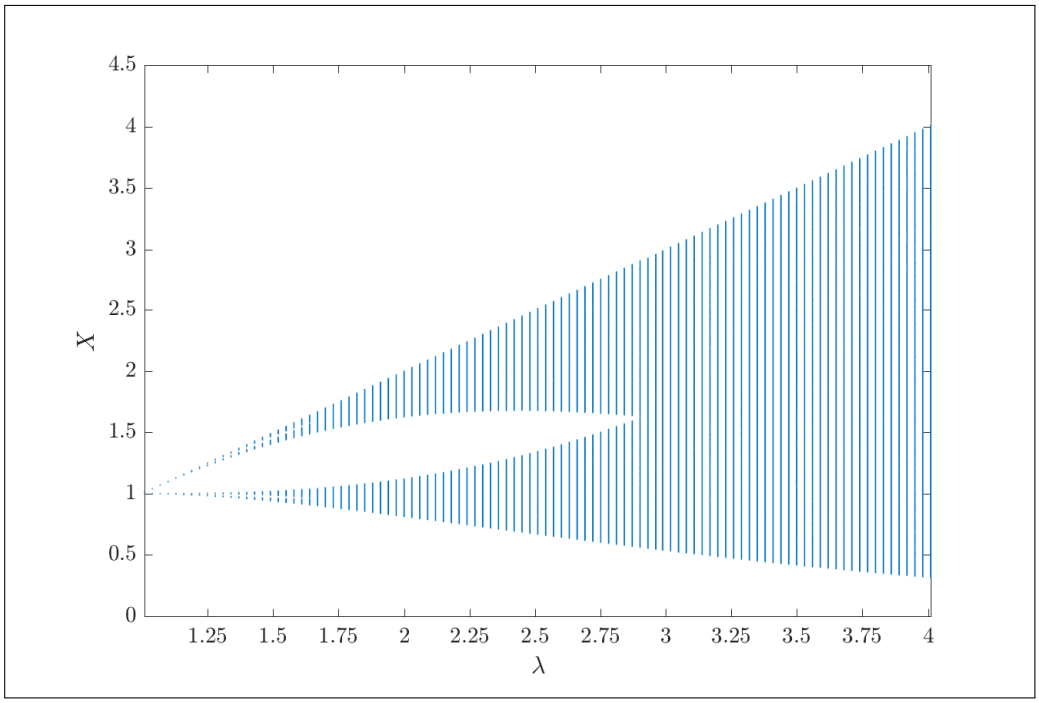

Figure 11: Bifurcation diagram of $F_\lambda(x) = \lambda x[1 - I(x)]$. We used 10000 data points.

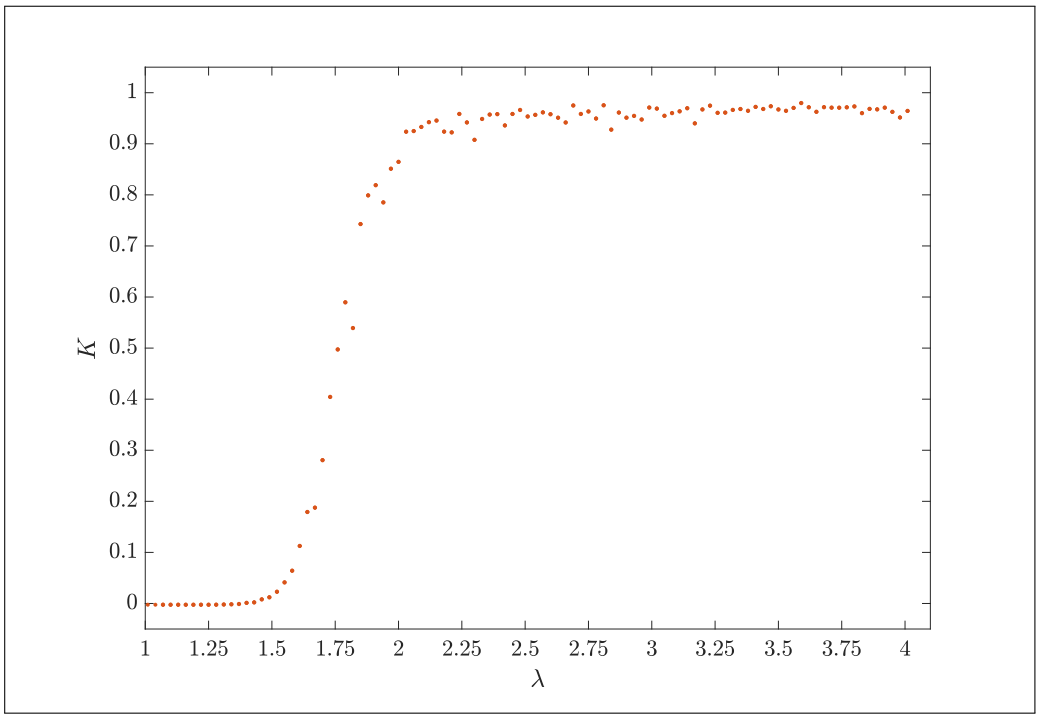

Figure 12: Plot of K versus λ for $F_\lambda(x) = \lambda x[1 - I(x)]$ calculated with 10000 data points and 100 values of $c \in [\pi/5, 4\pi/5]$. For regular dynamics, K is close to 0, for chaotic dynamics K is close to 1.

```
function model2plot(lambda,x0,N)

% lambda   parameter of the function
% x0       initial value of x
% N        number of iterations of the function

    x = zeros(N,1);
    x(1) = x0;
    for i = 1:1:N-1
        x(i+1)= lambda*x(i)*(1-model2I(x(i)));
    end
    plot(x(1:1:end-1),x(2:1:end),'.');
end
```

Listing 6: Plot of the model for discrete and nonoverlapping generations regulated by microparasites 15 in Matlab.

In the previous code, see Listing 6 the function model2I is called in order to calculate the value of the implicit function I shown on Listing 7 .

```
function[y] = model2I(x)
    syms I;
    f = exp(-I*x)+I-1;
    y = solve(f,I);
end
```

Listing 7: Code for solving the implicit equation in Matlab.

```
function[y] = model2F(x,lambda)
    y = lambda.*x.*(1-model2I(x));
end
```

Listing 8: Code of the equation of the model 15.

7 Conclusions

The goal of this thesis was the study of the 0-1 for chaos, a new method for distinguishing regular and chaotic dynamics in dynamical systems, introduced in [12], and its applications. The test was applied on two models from population biology, the Ricker model [39], and a model of populations with nonoverlapping generations regulated by microparasites, studied by R. M. May in [33]. The first model was in an explicit form, while the second one was described by an implicit equation.

After a brief introduction of the dynamical systems and the history of their study, an overview of application of the 0-1 test for chaos was given. This test was described in detail, together with its positives, among which we highlight its easy implementation, binary characteristic, the irrelevant nature of the system on which it is applied and direct application on data of all sorts.

The 0-1 test for chaos is implemented in Matlab (see Listing 1) and used on two models, (10) and (15). The output of this study of the dynamics is mainly in form of figures. For every model we can see a comparison of the plots for different values of their parameter (Figures 1 and 7), a cobweb diagram (in Figures 2 and 8) showing the nature of its fixed points, a bifurcation diagram (in Figures 5 and 11), and figures concerning the result of the 0-1 test for chaos.

In both cases we studied the boundedness of the trajectory in the (p, q)-plane in the plots of p_c versus q_c (see Figures 3 and 9), the relation between the control parameter of the test K_c and c (in Figures 4 and 10), and finally the final result of the test (in Figures 6 and 12), the control parameter K depending on the parameter of the function r or λ. This result was compared with the bifurcation diagram, and we can conclude that both methods gave comparable results.

We used a different size of data sample in the experiments, using only half of the data points N for the second model due to a longer computation time of the implicit function, clearly getting better results for higher values of N. Therefore, this is an issue for future research, along with the computation of the maximal Lyapunov exponents for our chosen models, to further compare the results from the 0-1 test for chaos with known methods for studying dynamical systems.

References

[1] D.V. Anosov and V.I. Arnold. *Dynamical Systems: Bifurcation theory and catastrophe theory*. Encyclopaedia of mathematical sciences. Springer-Verlag, 1994.

[2] J. Banks, J. Brooks, G. Cairns, G. Davis, and P. Stacey. On devaney's definition of chaos. *Am. Math. Monthly*, 99(4):332–334, April 1992.

[3] B.C. Bao, P.Y. Wu, H. Bao, Q. Xu, and M. Chen. Numerical and experimental confirmations of quasi-periodic behavior and chaotic bursting in third-order autonomous memristive oscillator. *Chaos, Solitons & Fractals*, 106:161 – 170, 2018.

[4] D. Bernardini and G. Litak. An overview of 0–1 test for chaos. *Journal of the Brazilian Society of Mechanical Sciences and Engineering*, 38(5):1433–1450, 2016.

[5] G. D. Birkhoff. Proof of the ergodic theorem. *Proceedings of the National Academy of Sciences*, 17(12):656–660, 1931.

[6] G.D. Birkhoff. Recent advances in dynamics. *Science*, 51(1307):51–55, 1920.

[7] J. Cao, A. Syta, G. Litak, S. Zhou, D.J. Inman, and Y. Chen. Regular and chaotic vibration in a piezoelectric energy harvester with fractional damping. *European Physical Journal Plus*, 130(6), 2015.

[8] R. L. Devaney. *An introduction to chaotic dynamical systems*. Addison-Wesley Publishing Company, 1987.

[9] S.-L. Ding, E.-Z. Song, L.-P. Yang, G. Litak, Y.-Y. Wang, C. Yao, and X.-Z. Ma. Analysis of chaos in the combustion process of premixed natural gas engine. *Applied Thermal Engineering*, 121:768 – 778, 2017.

[10] S.-L. Ding, E.-Z. Song, L.-P. Yang, G. Litak, C. Yao, and X.-Z. Ma. Investigation on nonlinear dynamic characteristics of combustion instability in the lean-burn premixed natural gas engine. *Chaos, Solitons & Fractals*, 93:99 – 110, 2016.

[11] J.S.A. Eyebe Fouda, B. Bodo, G.M.D. Djeufa, and S. L. Sabat. Experimental chaos detection in the duffing oscillator. *Communications in Nonlinear Science and Numerical Simulation*, 33:259 – 269, 2016.

[12] G.A. Gottwald and I. Melbourne. A new test for chaos in deterministic systems. *Proceedings of the Royal Society A: Mathematical, Physical and Engineering Sciences*, 460(2042):603–611, 2004.

[13] G.A. Gottwald and I. Melbourne. Testing for chaos in deterministic systems with noise. *Physica D: Nonlinear Phenomena*, 212(1-2):100–110, 2005.

[14] G.A. Gottwald and I. Melbourne. On the implementation of the 0-1 test for chaos. *SIAM Journal on Applied Dynamical Systems*, 8(1):129–145, 2009.

[15] G.A. Gottwald and I. Melbourne. On the validity of the 0-1 test for chaos. *Nonlinearity*, 22(6):1367–1382, 2009.

[16] R. Gu. Kato's chaos in set-valued discrete systems. *Chaos, Solitons and Fractals*, 31(3):765–771, 2007.

[17] J.L.G. Guirao and M. Lampart. Relations between distributional, li-yorke and ω chaos. *Chaos, Solitons and Fractals*, 28(3):788–792, 2006.

[18] Paul R. Halmos. Von neumann on measure and ergodic theory. *Bull. Amer. Math. Soc.*, 64:86–94, 05 1958.

[19] P. Harris, C.R. Bowen, H.A. Kim, and G. Litak. Dynamics of a vibrational energy harvester with a bistable beam: Voltage response identification by multiscale entropy and "0-1" test. *European Physical Journal Plus*, 131(4), 2016.

[20] M. Jazaeri and B. Honary. Block-coppels chaos in set-valued discrete systems. *Iranian Journal of Numerical Analysis and Optimization*, 3(1), 2013.

[21] M.H. Khondekar, D.N. Ghosh, K. Ghosh, and A.K. Bhattacharjee. Complexity in solar irradiance from the earth radiation budget satellite. *IEEE Systems Journal*, 9(2):487–494, 2015.

[22] M. Lampart. Two kinds of chaos and relations between them. *Acta Mathematica Universitatis Comenianae*, 72(1):119–127, 2003.

[23] M. Lampart. *Dynamical systems for geoinformatics*. Ostrava: VŠB - Technical University, 2013. ISBN: 978-80-248-2969-2.

[24] M. Lampart and J. Zapoměl. Dynamical properties of a non-autonomous bouncing ball model forced by non-harmonic excitation. *Mathematical Methods in the Applied Sciences*, 39(16):4923–4929, 2016.

[25] S. Li. ω-chaos and topological entropy. *Transactions of the American Mathematical Society*, 339(1):243–249, 1993.

[26] T.-Y. Li and J. A. Yorke. *Period Three Implies Chaos*, pages 77–84. Springer New York, New York, NY, 2004.

[27] G. Litak, D. Bernardini, A. Syta, G. Rega, and A. Rysak. Analysis of chaotic non-isothermal solutions of thermomechanical shape memory oscillators. *European Physical Journal: Special Topics*, 222(7):1637–1647, 2013.

[28] G. Litak, M.I. Friswell, and S. Adhikari. Regular and chaotic vibration in a piezoelectric energy harvester. *Meccanica*, 51(5):1017–1025, 2016.

[29] G. Litak, A. Syta, and M. Wiercigroch. Identification of chaos in a cutting process by the 0-1 test. *Chaos, Solitons and Fractals*, 40(5):2095–2101, 2009.

[30] D. Liu, Y. Xu, and J. Li. Randomly-disordered-periodic-induced chaos in a piezoelectric vibration energy harvester system with fractional-order physical properties. *Journal of Sound and Vibration*, 399:182 – 196, 2017.

[31] A.M. Lyapunov. The general problem of the stability of motion. *International Journal of Control*, 55(3):531–534, 1992.

[32] T. Martinovič. Chaotic behaviour of noisy traffic data. *Mathematical Methods in the Applied Sciences*, 41(6):2287–2293, 2018.

[33] R. M. May. Regulation of populations with nonoverlapping generations by microparasites: A purely chaotic system. *The American Naturalist*, 125(4):573–584, 1985.

[34] R. M. May. Chaos and the dynamics of biological populations. *Proceedings of The Royal Society of London, Series A: Mathematical and Physical Sciences*, 413(1844):27–44, 1987.

[35] M. Melosik and W. Marszalek. On the 0/1 test for chaos in continuous systems. *Bulletin of the Polish Academy of Sciences: Technical Sciences*, 64(3):521–528, 2016.

[36] M. Melosik and W. Marszalek. Using the 0-1 test for chaos to detect hardware trojans in chaotic bit generators. *Electronics Letters*, 52(11):919–921, 2016.

[37] M. Nicol, I. Melbourne, and P. Ashwin. Euclidean extensions of dynamical systems. *Nonlinearity*, 14(2):275–300, 2001.

[38] H. Poincaré and B.D. Popp. *The Three-Body Problem and the Equations of Dynamics: Poincaré's Foundational Work on Dynamical Systems Theory*. Springer International Publishing, 2017.

[39] W. E. Ricker. Stock and recruitment. *Journal of the Fisheries Research Board of Canada*, 11(5):559–623, 1954.

[40] H. Román-Flores and Y. Chalco-Cano. Robinson's chaos in set-valued discrete systems. *Chaos, Solitons & Fractals*, 25(1):33 – 42, 2005.

[41] M. A. Savi, F. H. I. Pereira-Pinto, F. M. Viola, A. S. de Paula, D. Bernardini, G., and G. Rega. Using 0-1 test to diagnose chaos on shape memory alloy dynamical systems. *Chaos, Solitons & Fractals*, 103:307 – 324, 2017.

[42] J. Smital and M. Kuchta. Two point scrambled set implies chaos. *(Proceedings of the European Conference of Iteration Theory, Spain 1987)*, pages 427–430, 1989.

[43] A. Syta, C.R. Bowen, H.A. Kim, A. Rysak, and G. Litak. Experimental analysis of the dynamical response of energy harvesting devices based on bistable laminated plates. *Meccanica*, 50(8):1961–1970, 2015.

[44] J. von Neumann. Proof of the quasi-ergodic hypothesis. *Proceedings of the National Academy of Sciences*, 18(1):70–82, 1932.

[45] Y. Wu. 1d bifurcation plot. `https://uk.mathworks.com/matlabcentral/fileexchange/26839-1d-bifurcation-plot`, 2010.

[46] E. Zambrano-Serrano, J.M. Munoz-Pacheco, and E. Campos-Canton. Chaos generation in fractional-order switched systems and its digital implementation. *AEU - International Journal of Electronics and Communications*, 79:43 – 52, 2017.

[47] M. Čiklová. Dynamical systems generated by functions with connected gδ graphs. *Real Analysis Exchange*, 30(2):617–638, 2004.

[48] M. Čiklová. Minimal and ω-minimal sets of functions with connected gδ graphs. *Real Analysis Exchange*, 32(2):397–408, 2007.